# Picosecond coherent Raman measurements of optical-phonon relaxation in $LaF_3:Ce^{3+}$

Claire L. Schosser* and Dana D. Dlott
*University of Illinois, School of Chemical Sciences, 505 South Mathews Avenue, Urbana, Illinois 61801*
(Received 3 April 1984)

An investigation of dephasing rates of some optical phonons in $LaF_3:Ce^{3+}$ (2 at. % $Ce^{3+}$) crystals by picosecond time-resolved coherent anti-Stokes Raman spectroscopy is presented. At low temperature the lifetime of the 78-$cm^{-1}$ phonon is 380 ps, while those of five other phonons of $>200$ $cm^{-1}$ energy are in the range $2 < T_1 < 10$ ps. The decay of the 78-$cm^{-1}$ phonon is due to anharmonic spontaneous emission of two 39-$cm^{-1}$ optical phonons with a cubic anharmonic matrix element $\langle B^{(3)}{}^{0}_{78}{}^{k}_{39}{}^{-k}_{39}\rangle = 0.15 \pm 0.05$ $cm^{-1}$. The decay of the other phonons studied likely occurs by an analogous process. The matrix elements for these phonons appear to be in the range 0.2—0.6 $cm^{-1}$. The dephasing rate of the 78-$cm^{-1}$ phonon is followed as a function of temperature to $\sim 100$ K, and the rates are well fitted by an energy relaxation model involving emission to 39-$cm^{-1}$ phonons and absorption of $\sim 40$ and $\sim 118$-$cm^{-1}$ thermally excited phonons. The matrix elements for absorption processes are $(0.3 \pm 0.1)$ and $(0.5 \pm 0.2)$ $cm^{-1}$, respectively. The rate of absorption of thermally excited 78-$cm^{-1}$ phonons is $< 10\%$ of the rate of the other up-conversion processes, and it is suggested that this is due to a type of symmetry selection rule for phonon-phonon scattering arising from small distortions away from a bimolecular unit cell to a hexamolecular cell, which creates two distinct types of phonons.

## I. INTRODUCTION

In this paper we discuss picosecond coherent anti-Stokes Raman spectroscopy (ps CARS) measurements of optical-phonon dynamics[1-3] in $LaF_3:Ce^{3+}$ crystals. Since $LaF_3$ is often used as a host crystal for studying electronic energy transitions in a variety of impurity rare-earth ions,[4] a knowledge of the phonon dynamics is crucial for understanding electron-phonon coupling caused by interactions of the $4f$ impurity electrons with the host-crystal phonons.[5] These interactions create phonon sidebands[5] and affect the homogeneous linewidth of the electronic transition.[6] A knowledge of phonon-phonon interactions is crucial to the understanding of thermal conductivity, and possibly also to the ionic conductivity[7] that has been observed in $LaF_3$. $LaF_3$ is also a technologically important material which is used as a host crystal in several types of solid-state lasers.[4] A knowledge of phonon dynamics here can add to an understanding of nonradiative relaxation that occurs during the pumping of the laser. Doped $LaF_3$ has been used as a phonon spectrometer[8] utilizing various impurity ions and phonon-generation and -detection schemes. In these experiments high-wave-vector acoustic or optical phonons of $LaF_3$ are generated and detected by phonon coupling to electronic transitions of rare-earth ions. The results obtained by ps CARS extend the information available for $\vec{k} \approx \vec{0}$ optical phonons of higher energies ($\geq 78$ $cm^{-1}$) and allow for a fuller characterization of phonon dynamics without the complication of indirect generation and detection.

In the previous studies of the decay of large wave-vector acoustic phonons in $LaF_3$, acoustic phonons of 23 $cm^{-1}$ energy were studied in $LaF_3:Pr^{3+}$ where the $Pr^{3+}$ concentration is 0.05 at. %.[9] It was observed that the lifetime of these phonons was $\sim 200$ ns. Sox, Rives, and Meltzer used stimulated emission of phonons generated by the relaxation between the Kramers components of $Er^{3+}$ to study 5- and 7-$cm^{-1}$ phonons in $LaF_3:Er^{3+}$ with 0.1 at. % $Er^{3+}$ and obtained spin-lattice relaxation times of 46 and 6.2 $\mu$s, respectively.[10] Will *et al.* used a heat-pulse technique and fluorescence detection to examine lifetimes of phonons in $LaF_3:Er^{3+}$ (0.05 at. % $Er^{3+}$) of energies from $\sim 13$ to $\sim 30$ $cm^{-1}$ and observed lifetimes in the (50—1000)-ns range.[11] Above 20 $cm^{-1}$ they observed a $\nu^{-5}$ dependence of the lifetime on the phonon frequency. Very recently, Meltzer, Rives, and Dixon used vibronic sideband phonon spectroscopy to examine phonons in $LaF_3:Er^{3+}$, $Pr^{3+}$ (0.5 at. % $Pr^{3+}$, 0.3 at. % $Er^{3+}$) of energies of 41 and 54 $cm^{-1}$.[12] The authors argue on the basis of a partial dispersion curve[13] obtained for $LaF_3$ in the course of that study that the 41- and 54-$cm^{-1}$ phonons created are primarily optical phonons and that their decay is dominated by anharmonic emission of two lower-energy phonons. The decay times obtained for the 41- and 54-$cm^{-1}$ phonons are $\sim 40$ and $\sim 5$ ns, respectively.

We have previously used the ps CARS technique to study optical-phonon relaxation in a variety of molecular solids including the aromatic hydrocarbon naphthalene,[3,14] the amino acid *l*-alanine,[15] and, most recently, a variety of amino acid and peptide crystals.[16] In naphthalene, the intermolecular interactions are all due to weak van der Waals forces. In the amino acids and peptides the majority of intermolecular interactions are of this type, but there are also several strong hydrogen bonds at each molecule. In the ps CARS technique a $\vec{k} \approx \vec{0}$ optical phonon of frequency $\Omega$ is coherently excited by two simultaneous picosecond pulses of frequencies

 

$\omega_1-\omega_2=\Omega$. The coherent anti-Stokes emission at $\Omega+\omega_1$, stimulated by a delayed $\omega_1$ pulse, is detected as the delay is varied. The coherent anti-Stokes emission decays due to phonon dephasing, which is also responsible for the finite width of the optical line shape. This technique is particularly suited for studying long-lived phonons ($T_1 > 10$ ps) in solids.

In solids at low temperature there are two important phonon-dephasing mechanisms.[1,2,3,17] Phonon relaxation by anharmonic decay into lower-frequency modes results in homogeneous broadening, giving Lorentzian lines in the frequency domain and an exponential decay of the ps CARS signal.[17] Phonon scattering from static defects in the crystal[7] causes inhomogeneous broadening which results in a nonexponential ps CARS decay.[18]

The lowest-frequency totally symmetric optical phonons in naphthalene and perdeuteronaphthalene (69 and 64 $cm^{-1}$, respectively) show no detectable inhomogeneous broadening at 1.5 K, so the ps CARS decay yields a lifetime of 120 ps.[14] The depopulation is apparently caused by spontaneous emission of two acoustic phonons at half the optical-phonon frequency.[1,14,19] The rate of such processes is proportional to the sum of the squares of the various cubic anharmonic matrix elements ($B$ coefficients) for each decay pathway which conserves energy and wave vector.[20,21] A recent lattice-dynamical calculation of these matrix elements for naphthalene showed them to be nearly equal (within a factor of $\sim 5$) for each decay pathway of the nine optical phonons, and thus optical-phonon lifetimes are primarily determined by the two-phonon density of states.[21] This type of calculation can only be performed on those few crystals for which detailed dispersion relations and one-phonon state densities have been obtained from neutron scattering. In addition, the procedure involves lengthy computations. Since we want to study a variety of interesting complex materials, we investigated a simplified model which assumes the $B$ coefficients all equal to an average value.[14] In this model, the low-temperature optical-phonon lifetimes and the temperature dependence of the lifetimes are fitted with one adjustable parameter, the average cubic anharmonicity. This model is in excellent agreement with the temperature dependence of the naphthalene phonon lifetime from 1.5 to 200 K. In $l$-alanine we measured the lifetimes of seven optical phonons and the temperature dependences.[15,16] These data were also in good agreement with this model. The average $B$ coefficient was $\sim 3$ $cm^{-1}$ in both materials. This value is similar in both types of crystals because the H bonds in $l$-alanine do not contribute much to the anharmonic potential, and the rest of the intermolecular interactions (of the nonbonded C—C, C—H, and H—H type) are quite similar, as evidenced by x-ray studies of bond lengths.[22]

The $LaF_3$ crystal structure has been the subject of some controversy, which appears to have been resolved. The unit cell is nearly bimolecular in the $D^4_{6h}$ factor group[23(a)] but small distortions lower the symmetry to a hexamolecular cell of $D^4_{3d}$ symmetry.[23(a),24,25] There are thus two distinct types of optical phonons in the crystal, 21 which arise from the bimolecular cell, and 48 which occur solely as a result of the distortion. We will call these $B$ or $H$ phonons, respectively. Since the distortion is slight, the $B$ phonons show the most intense optical transitions.[23] We observe four of the five Raman-active phonons of this type. The lowest of these modes, at 78 $cm^{-1}$, is long lived ($T_1 \sim 400$ ps) in $LaF_3$:$Ce^{3+}$(2 at. %) at low temperature, whereas the other three decay more rapidly ($T_1 < 10$ ps). These results are consistent with the energy-relaxation model for an anharmonic matrix element about an order of magnitude smaller than naphthalene. The smaller anharmonicity is the result of strong ionic interactions, compared to weak nonbonded interactions in naphthalene, and correlates well with another measure of anharmonicity—pressure-dependent phonon-frequency shifts.

At low temperature the 78-$cm^{-1}$ mode decays to two counterpropagating 39-$cm^{-1}$ phonons. If the crystal were bimolecular, only acoustic phonons would exist at 39 $cm^{-1}$. Since the Debye frequency of $LaF_3$ is high,[26] the acoustic-phonon density of states is small. Dixon and Nicklow have shown, on the basis of neutron-diffraction data, that a Raman-active $\vec{k} \approx \vec{0}$ phonon exists at $\sim 40$ $cm^{-1}$.[13] This mode is not observed in the Raman spectrum or in our CARS measurement, and it undoubtably is an $H$ phonon. The dispersion of this mode is small, resulting in a large density of optical states at this frequency. The 78-$cm^{-1}$ mode decays primarily to these optical phonons. Thus, in an important sense the lattice distortion controls the 78-$cm^{-1}$ phonon lifetime. The temperature-dependent line broadening is studied in detail to $\sim 100$ K. The temperature dependence is dominated by absorption of optical phonons (up conversion) at $\sim 40$ and $\sim 118$ $cm^{-1}$. We do not see an appreciable contribution from the process 78 $cm^{-1}$ + 78 $cm^{-1}$ → approximately 160 $cm^{-1}$, although there is considerable state density at 160 $cm^{-1}$. Either the dispersion of the final phonons does not permit $\vec{k}$-vector matching or the phonon-phonon scattering is governed by a selection rule which arises because there are two types of phonons, the $B$ and $H$ types.

## II. EXPERIMENTAL RESULTS

The $LaF_3$ crystals of several $mm^3$ dimensions were obtained from Dr. W. Hargreaves of Optovac Inc. One crystal was cut in pieces in order to study the orientation dependence of the CARS intensity. Although the intensities change with orientation, we observed the same phonons and decay rates in each geometry. The detailed ps CARS results were obtained on $\sim 1$-mm-thick samples of $LaF_3$:$Ce^{3+}$(2 at. %) oriented with the $c$ axis normal to the crystal faces and in the direction of propagation of the laser beams. $Ce^{3+}$ was chosen because it has no significant absorption at the dye-laser wavelengths (5550—5650 Å).[4] Some experiments were also performed on undoped $LaF_3$. The ps CARS apparatus, consisting of two dye lasers pumped by a high-repetition-rate Nd:YAG laser (YAG denotes yttrium aluminum garnet), has been described previously.[3(b)] This experiment measures vibrational dephasing in the time domain. The decay of the ps CARS signal is given by

$$I(t) \propto |\langle q(0)q(t)\rangle|^2 , \quad (1)$$

where $q(t)$ is the value of the phonon normal coordinate.[18] The ps CARS decay is thus proportional to the absolute square of the correlation function.

In a crystal at low temperature there is a natural separation of time scales for phonon dynamics. The only "fast" process is spontaneous emission of lower-frequency phonons, and thus the low-temperature homogeneous optical linewidth is due solely to the lifetime.[17] Other interactions such as scattering from defects or impurities are essentially static and give rise to additional inhomogeneous broadening (pure phase relaxation). The effects of these scattering mechanisms are discussed in Ref. 8. For simplicity we adopt a phenomenological model where the distribution of scattering rates is random with standard deviation $\sigma_t$. Then the phonon optical line shape is described by the Voight profile[27] given by

$$I(t) \propto \exp(-t/T_1)\exp(-t^2/2\sigma_t^2) , \quad (2)$$

where $T_1$ is the phonon lifetime. Equation (2) is the time-domain Voight line shape. When $(T_1)^{-1}\sigma_t \gg 1$, exponential decays are observed and inhomogeneous broadening is negligible. In this case the Raman line shape is Lorentzian with width $\Delta\nu$ given by[27]

$$\Delta\nu\ (\mathrm{cm}^{-1}) = \frac{5.33}{T_1\ (\mathrm{ps})} . \quad (3)$$

Several Raman-active phonons in $LaF_3$ were located by CARS spectroscopy. Although this technique produces intense coherent emission, the sensitivity is limited by our ability to discriminate against the nonresonant background scattering at the same frequency. Strong phonon transitions were observed at 78, 314, 365, and 390 $cm^{-1}$, and somewhat weaker phonon transitions were observed at 203 and 230 $cm^{-1}$. This is in agreement with the expectation that the phonon transitions at 203 and 230 $cm^{-1}$, which exist only due to the small symmetry-breaking interactions, should have a smaller transition moment than the modes derived mainly from the bimolecular structure.[23] We could not discern any phonon in the 40-$cm^{-1}$ range above the nonresonant background. Our inability to observe the 40-$cm^{-1}$ mode would indicate that it is likely to be a low-intensity mode that is present due to the slight distortion if the argument advanced by Dixon and Nicklow[13] (that the 40-$cm^{-1}$ mode must be Raman active if the ir assignments are assumed to be correct) is valid.

At low temperature all of these phonons (except the 78-$cm^{-1}$ mode) showed decays identical to the instrumental response. For these modes, $T_1 \lesssim 10$ ps and $\Delta\nu \gtrsim 0.5$ $cm^{-1}$. In all samples the 78-$cm^{-1}$ mode decayed much more slowly. The temperature dependence was studied in detail. Most of the experiments were performed in a variable-temperature closed-cycle refrigerator (9—320 K) with the crystal in thermal contact to a copper block. One run was performed with a crystal immersed in 1.5-K superfluid helium and held in a strain-free mounting (a small aluminum-foil envelope). The decays in this case were identical to the 9-K refrigerator data, indicating that strain in the crystal mounting did not affect the crystal in

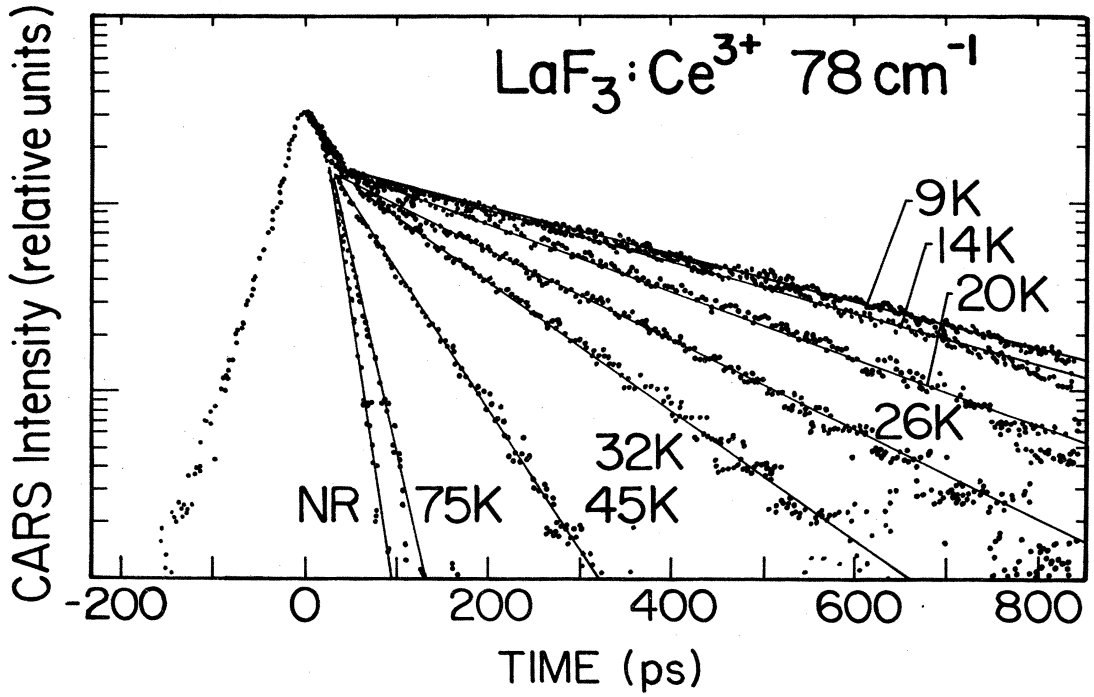


FIG. 1. Semilogarithmic plots of ps CARS decays of 78-$cm^{-1}$ optical phonon in $LaF_3$:$Ce^{3+}$ crystal at different temperatures. The decays are nearly exponential, with the inhomogeneous linewidth $< 10\%$ of the homogeneous linewidth at 9 K. The lifetime at 9 K is (380±20) ps. The decay labeled NR (nonresonant) is the instrumental response function obtained by tuning one laser $\sim 15$ $cm^{-1}$ off the 78-$cm^{-1}$ signal.

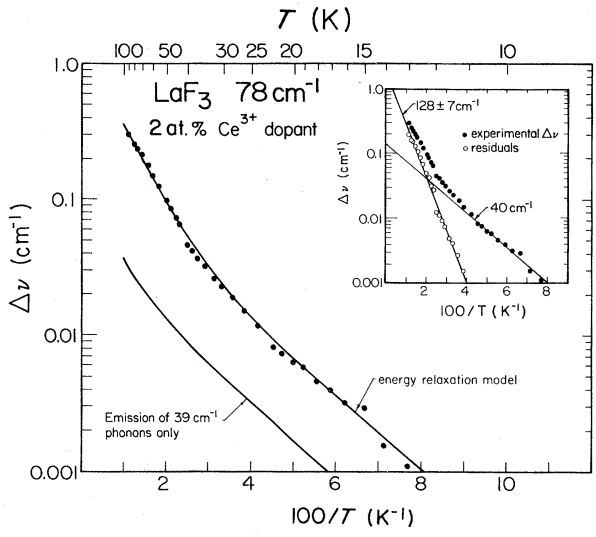


FIG. 2. Temperature dependence of the linewidth of the 78-$cm^{-1}$ optical phonon in $LaF_3$ obtained from the ps CARS data. The data are plotted as the linewidth at temperature $T$ minus the low-temperature linewidth versus $1/T$. The temperature dependence of an undoped $LaF_3$ sample is found to be similar. The solid lines are calculated temperature dependences obtained using Eqs. (6), (8), and (9) for stimulated emission to 39-$cm^{-1}$ phonons only, and for that process plus up conversion involving $\sim$40- and $\sim$118-$cm^{-1}$ thermally excited phonons, with no contribution involving scattering by thermally excited 78-$cm^{-1}$ phonons. The inset shows that the data may be well described by a sum of two exponentials, one of slope 40 $cm^{-1}$ and one of slope (128±7) $cm^{-1}$.

the refrigerator, and that the lowest temperature obtainable in the refrigerator (9 K) was sufficient to freeze out most thermal line broadening. The 78-$cm^{-1}$ phonon in our two undoped $LaF_3$ samples decayed somewhat faster than in $LaF_3$:$Ce^{3+}$, which suggests that a concentration study would be interesting.

In Fig. 1 we show a series of ps CARS decays of the $LaF_3$:$Ce^{3+}$(2 at.%) crystal at various temperatures. The initial rapid transient at $t=0$ is due to the nonresonant susceptibility.[1,2] The decays are very nearly exponential at all temperatures. At 9 K the lifetime is (380±20) ps, corresponding to a Lorentzian linewidth of (0.0140±0.0007) $cm^{-1}$. By a computer fit of the data to Eq. (2), we determined that the inhomogeneous linewidth at 9 K is less than $10^{-3}$ $cm^{-1}$ despite the 2 at.% doping level. The decay marked NR (nonresonant) in Fig. 1 is the measured instrumental response of the laser system obtained by tuning one laser $\sim$15 $cm^{-1}$ away from 78 $cm^{-1}$. The trailing edge is exponential with $1/e$ decay lifetime of (14±0.5) ps. A decay with $T_1 > 10$ ps would result in noticeable broadening of this function.

Figure 2 shows the temperature dependence of the linewidth for the data (solid circles) from Fig. 1. We plot $\Delta\nu$, the linewidth with the 9-K value subtracted, versus the inverse temperature. Undoped $LaF_3$ shows a very similar temperature dependence to the 2-at.% $Ce^{3+}$ crystal. From 9 to 90 K the linewidth change is seen to vary over a dynamic range of $\sim 3\times 10^2$. The calculated curves are a fit to the energy-relaxation model discussed in the next section. The data are nonlinear over this temperature range and indicate that more than one phonon is involved in the relaxation process. The inset shows that the initial (low-temperature) slope of the data is 40 $cm^{-1}$. The residuals (open circles in inset) are linear ($r > -0.99$) with a slope of (128±7) $cm^{-1}$. Thus the temperature dependence is approximated quite well in this regime by a sum of two exponentials.

## III. DISCUSSION

The lack of substantial inhomogeneous broadening observed for the 78-$cm^{-1}$ phonon in the $LaF_3$:$Ce^{3+}$(2 at.%) indicates that at low temperatures vibrational dephasing is dominated by energy relaxation through spontaneous emission of phonons. The defect scattering rate in the 2-at.% doped crystal is apparently less than $5\times 10^8$ $s^{-1}$. Consequently, only the longer-lived, lower-frequency phonons should be strongly affected by defects. The rate of energy relaxation can be calculated by expanding the crystal potential energy about the equilibrium position in powers of the phonon normal coordinates.[20,21] The temperature dependence (Fig. 2), which has an initial slope of $\sim$40 $cm^{-1}$, indicates that only two phonons are emitted in the decay process. (Multiphonon emission would show a steeper temperature dependence.[1]) In this case the temperature-dependent lifetime $T_1(T)$ of a laser-generated phonon, whose frequency is $\Omega$ and wave vector $\vec{k}\approx\vec{0}$, is[21]

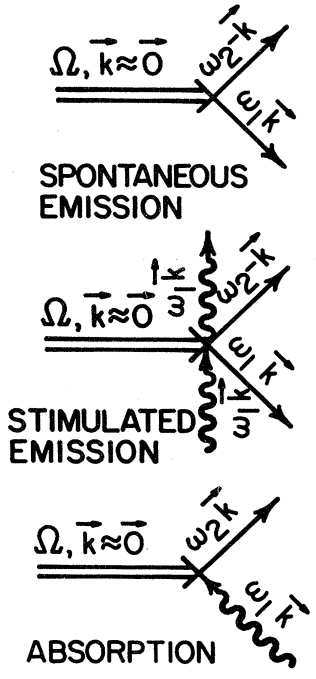


FIG. 3. Diagrammatic representation of phonon decay caused by cubic anharmonic coupling. The double solid lines represent a laser-generated phonon, single solid lines represent emitted phonons, and wavy lines represent thermal phonons. Only one stimulated-emission diagram is shown; in the other diagram the emission is stimulated by an $\omega_2$ phonon.

$$[T_1(T)]^{-1}_{\Omega,\vec{k}\approx\vec{0}}=\frac{36}{\hbar^2}\sum_{\omega_1,\omega_2}\left[\left\langle B^{(3)}\ \begin{matrix}\vec{0}&\vec{k}&-\vec{k}\\ \Omega&\omega_1&\omega_2\end{matrix}\right\rangle^2(n_{\omega_1}+n_{\omega_2}+1)\delta(\Omega-\omega_1-\omega_2)+\left\langle B^{(3)}\ \begin{matrix}\vec{0}&\vec{k}&\vec{k}\\ \Omega&\omega_1&\omega_2\end{matrix}\right\rangle^2(n_{\omega_1}-n_{\omega_2})\delta(\Omega+\omega_1-\omega_2)\right], \tag{4a}$$

where

$$n_\omega=[\exp(\hbar\omega/k_BT)-1]^{-1} \tag{4b}$$

is the thermal occupation number of phonons of frequency $\omega$, and the $B$ coefficients are defined in Ref. 21. Equation (4a) describes three distinct decay processes: spontaneous and stimulated emission, which result in down conversion to lower-frequency phonons $\omega_1$ and $\omega_2$, and absorption of $\omega_1$ phonons, which results in up conversion to an $\omega_2$ phonon. These processes are represented diagrammatically in Fig. 3. In the diagrams, a double arrow represents the laser-excited phonon, a wavy arrow a thermal phonon, and a single arrow an emitted phonon. Only one of the stimulated-emission diagrams is shown. The other would be identical except that a thermal $\omega_2$ phonon causes the relaxation.

In this work we wish to investigate the relation between the one-phonon density of states and the phonon decay rates. Since we lack a full dispersion-curve analysis for $LaF_3$ [the published dispersion curves extend to only $\sim 90$ $cm^{-1}$ (Ref. 13)], we consider only processes which can connect the $\vec{k}\approx\vec{0}$ phonons seen in ir and Raman investigations. In the absence of more detailed direction-dependent dispersions, the crystal is treated as an isotropic solid. Then Eq. (4a) is written as a sum over allowed decay processes. It is also necessary to know the two-phonon density of states. This quantity has been calculated for crystalline $NH_3$ (Ref. 20) and naphthalene (Ref. 21), and a reasonable approximation is the product of two one-phonon densities of states, i.e.,

$$\rho^{(2)}(\omega_1,\omega_2)\cong\rho(\omega_1)\rho(\omega_2)\ . \tag{5}$$

In this case Eq. (4b) becomes

$$[T_1(T)]^{-1}_{\Omega,\vec{k}\approx\vec{0}}=\frac{36}{\hbar^2}\sum_{\rm DC}\left\langle B^{(3)}\ \begin{matrix}\vec{0}&\vec{k}&-\vec{k}\\ \Omega&\omega_1&\Omega-\omega_1\end{matrix}\right\rangle^2(n_{\omega_1}+n_{\Omega-\omega_1}+1)\rho(\omega_1)\rho(\Omega-\omega_1)+\frac{36}{\hbar^2}\sum_{\rm UC}\left\langle B^{(3)}\ \begin{matrix}\vec{0}&\vec{k}&\vec{k}\\ \Omega&\omega_1&\omega_1+\Omega\end{matrix}\right\rangle^2(n_{\omega_1}-n_{\omega_1+\Omega})\rho(\omega_1)\rho(\omega_1+\Omega)\ , \tag{6}$$

where DC and UC indicate, respectively, down- and up-conversion processes.

For the 78-$cm^{-1}$ phonon, $[T_1(0)]_{78\ cm^{-1}}=380$ ps. There are two possible down-conversion processes: emission of two counterpropagating acoustic phonons at 39 $cm^{-1}$ or emission of two counterpropagating 39-$cm^{-1}$ optical phonons. The acoustic density of states can be calculated in the Debye approximation[27] ($\omega_D=272$ $cm^{-1}$ for low-temperature $LaF_3$).[26] Thus the low-temperature lifetime of the 78-$cm^{-1}$ mode is

$$[T_1(0)]^{-1}_{78\ cm^{-1}}=\frac{36}{\hbar^2}\left\langle B^{(3)}\ \begin{matrix}\vec{0}&\vec{k}&-\vec{k}\\ 78&39&39\end{matrix}\right\rangle^2_{\rm ac}\left[\frac{3\sqrt{6}(39)^2}{\omega_D^3}\right]^2+\frac{36}{\hbar^2}\left\langle B^{(3)}\ \begin{matrix}\vec{0}&\vec{k}&-\vec{k}\\ 78&39&39\end{matrix}\right\rangle^2_{\rm opt}(\rho^{\rm opt}_{39})^2\ , \tag{7}$$

where all frequencies are in $cm^{-1}$. Meltzer, Rives, and Dixon have approximated the density of states at $\sim 39$ $cm^{-1}$ and find that the optical modes dominate the acoustic-mode density at this frequency.[12] We estimate the optical density by noting there are two TO modes with an approximate bandwidth of 15 $cm^{-1}$ yielding $(\rho^{\rm opt}_{39})\simeq 0.13$ states/$cm^{-1}$. (The estimate used in Ref. 12 is identical.) Using Eq. (5) and the isotropic Debye approximation,[27] we find that the two-phonon optical density of states at 39 $cm^{-1}$ exceeds the acoustic contribution by $\sim 10^4$. Hence we conclude that the 78-$cm^{-1}$ mode decays primarily by optical-phonon emission, and we obtain

$$\left\langle B^{(3)}\ \begin{matrix}\vec{0}&\vec{k}&-\vec{k}\\ 78&39&39\end{matrix}\right\rangle_{\rm opt}=(0.15\pm 0.05)\ cm^{-1}\ . \tag{8}$$

If we had assumed instead that the decay was to acoustic phonons, the $B$ coefficient would be $\sim 35$ $cm^{-1}$, which is unrealistically large, being $\sim 50\%$ of the phonon frequency. The decay to optical phonons is caused by two effects: the small symmetry distortion which creates the hexamolecular unit cell and the 48 new optical phonons, and the high Debye frequency of $LaF_3$. The 78-$cm^{-1}$ mode and $\sim 40$-$cm^{-1}$ acoustic and optical phonons are illustrated schematically in Fig. 4. Although the phonon eigenvectors are not known exactly, the 78-$cm^{-1}$ mode is primarily a $La^{3+}$ translation[23(a)] with the two $La^{3+}$ ions in the unit cell moving out of phase. The illustration of the crystal is analogous to our experimental geometry: the crystal $c$ axis is out of plane and the $\vec{k}$ vector of the laser-generated 78-$cm^{-1}$ phonon is along the $a$ axis. For clarity, the $F^-$ ions are omitted and only one component

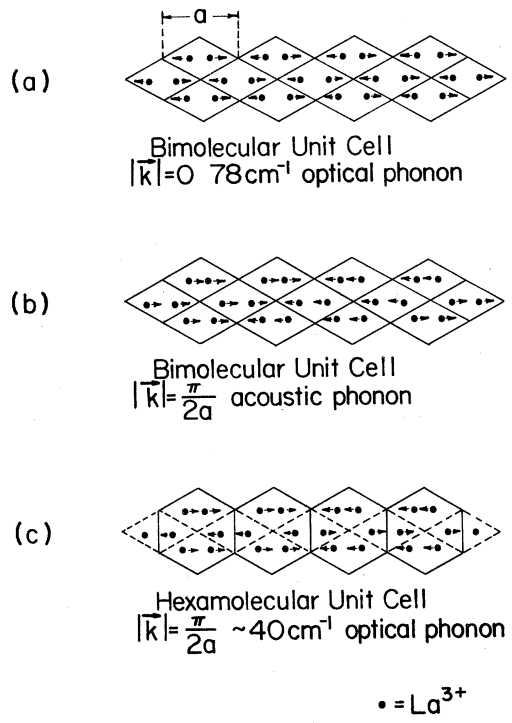


FIG. 4. Schematic representation of the phonons involved in the low-temperature decay of the 78-cm$^{-1}$ mode. Only the $La^{3+}$ ions and a component of motion in the horizontal direction are shown for clarity. The crystal $c$ axis is out of the page. (a) The $\vec{k}\approx\vec{0}$ 78-cm$^{-1}$ phonon is primarily a $La^{3+}$ motion. (b) An acoustic phonon of $|\vec{k}|=\pi/2a$ is shown. The actual phonon which can be emitted by the 78-cm$^{-1}$ mode has $|\vec{k}|\approx\pi/10a$. Dispersion of acoustic phonons in $LaF_3$ is large, resulting in a small acoustic density of states at 39 cm$^{-1}$. (c) The 40-cm$^{-1}$ optical phonon is created from acoustic phonons by the small symmetry-breaking distortion which creates the hexamolecular unit cell. This mode has very weak optical activity but has a large density of states at 39 cm$^{-1}$. Consequently, emission of two counterpropagating optical phonons accounts for most of the lifetime of the 78-cm$^{-1}$ mode.

of $La^{3+}$ motion is shown. Figure 4(a) illustrates the 78-cm$^{-1}$ $\vec{k}\approx\vec{0}$ mode for a hypothetical bimolecular $D_{4h}^6$ crystal. Figure 4(b) illustrates an acoustic phonon in the bimolecular crystal with $\vec{k}$ vector parallel to the $a$ axis and $|\vec{k}|=\pi/2a$. The actual acoustic phonons which would be emitted by the 78-cm$^{-1}$ mode have $|\vec{k}|\approx\pi/10a$. The out-of-phase interactions between adjacent unit cells are quite large and thus the phonon has a large dispersion resulting in a small density of states at about 40 cm$^{-1}$. Figure 4(c) illustrates the ~40-cm$^{-1}$ optical phonon in the hexamolecular cell. We have constructed what appears to be the lowest-frequency optic phonon in the hexamolecular cell. For illustrative purposes the outlines of the bimolecular cells are shown as dashed lines. The mode illustrated has $|k|=\pi/2a$, but we do not know the wavelength of the emitted phonons. If not for the lattice distortion, this mode would be an optically inactive acoustic phonon; consequently, it is not strongly optically active in the $LaF_3$ crystal. Since the dispersion of this mode is much smaller than for acoustic phonons,[13] the out-of-phase interaction between adjacent hexamolecular unit cells is relatively small, and there is considerable density of states at 39 cm$^{-1}$.

The temperature-dependent scattering processes of the 78-cm$^{-1}$ mode can now be analyzed using the data in Fig. 2. Since the ps CARS decays are exponential up to ~100 K, it is likely that the temperature dependence is due to a decreasing lifetime with temperature, although some contribution from "pure" dephasing cannot be ruled out. Recently, it was shown that the temperature dependence of naphthalene[14] and several amino-acid and peptide crystals[15,16] in this range is the result of energy relaxation. With the use of Eqs. (8) and (6) the rate of stimulated optical-phonon emission can be calculated with no adjustable parameters, and this rate is plotted in Fig. 2. This process, which has a 39-cm$^{-1}$ activation energy, accounts for only ~10% of the observed thermal line broadening, and we conclude that as in organic molecular crystals the up-conversion process is more efficient than down conversion.[1,19] Since up conversion involves scattering by $|\vec{k}|\neq0$ phonons, we initially expected that the 78-cm$^{-1}$ mode could interact with optical phonons of any symmetry (as discussed above, acoustic scattering is negligible), and that as the temperature was increased toward 100 K we would see scattering by all the low-frequency phonons

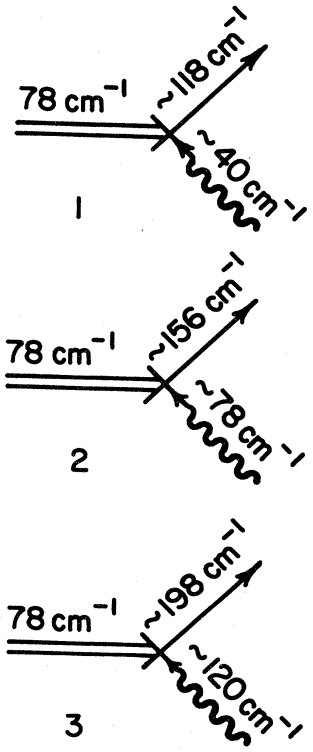


FIG. 5. Diagrammatic representation of the up-conversion processes most likely to affect the 78-cm$^{-1}$ phonon from 10—100 K. Process 2 is observed to be much less efficient than processes 1 and 3.

weighted appropriately by the thermal occupation numbers and density of states. The important up-conversion processes in this temperature range are shown in Fig. 5.

As is evident from Fig. 2 we see processes 1 and 3 but no sizable contribution from process 2. (Error analysis shows the rate of process 2 to be less than 10% of the other two processes.) The calculated temperature dependence in Fig. 2 is obtained by fitting Eq. (6) to the data. Two adjustable parameters were used: the efficiencies of the processes 1 and 3, defined as the product of the square of the $B$ coefficient and the density of states. As discussed above the calculation of the stimulated-emission rate requires no adjustable parameters.

The $B$ coefficients can be determined from these efficiencies if the appropriate values of the density of states are known. An approximate density of states for $LaF_3$ has been obtained by an analysis of phonon sidebands of the $^3H_4 \rightarrow {}^3P_0$ transition of $Pr^{3+}$ in 1 at.% $LaF_3$:$Pr^{3+}$.[5] We normalized the values of this density of states by ratioing them to the value obtained at 39 $cm^{-1}$. The relevant values of the density of states used in this work are given in Table I. The uncertainty in these values is estimated at 50% and is caused by our initial estimate of $\rho(39\ cm^{-1})$ and the effect of a variation of electron-phonon—coupling coefficients in the evaluation of the approximate density of states from Ref. 5. The values we obtain for the $B$ coefficients for up conversion of the 78-$cm^{-1}$ phonon are

$$\left\langle B^{(3)} \begin{matrix} \vec{0} & \vec{k} & \vec{k} \\ 78 & 40 & 128 \end{matrix} \right\rangle = (0.3 \pm 0.1)\ cm^{-1}\ , \tag{9a}$$

$$\left\langle B^{(3)} \begin{matrix} \vec{0} & \vec{k} & \vec{k} \\ 78 & 78 & 156 \end{matrix} \right\rangle < 0.08\ cm^{-1}\ , \tag{9b}$$

$$\left\langle B^{(3)} \begin{matrix} \vec{0} & \vec{k} & \vec{k} \\ 78 & 118 & 196 \end{matrix} \right\rangle = (0.5 \pm 0.2)\ cm^{-1}\ . \tag{9c}$$

TABLE I. One-phonon density of states for phonons involved in decay processes of optical phonons of $LaF_3$. Estimated uncertainty is 50%.

| $\omega$ ($cm^{-1}$) | $\rho(\omega)$ (states/$cm^{-1}$)[a] |
|---|---|
| 39 | 0.13 |
| 53 | 0.58 |
| 57 | 1.1 |
| 68 | 0.52 |
| 78 | 0.38 |
| 118 | 0.22 |
| 140 | 0.46 |
| 150 | 0.64 |
| 156 | 0.35 |
| 173 | 0.61 |
| 196 | 0.49 |
| 225 | 1.2 |
| 240 | 0.98 |
| 246 | 1.1 |

[a]To convert to the units used in Ref. 12 (states/$cm^{-1}$)/$cm^3$, multiply by $3 \times 10^{21}$.

ps CARS measurements were made on five other Raman-active phonons in $LaF_3$ at low temperature. These include three of the other four $B$-type phonons which are more intense than $H$-type phonons arising from the small lattice distortions. The ps CARS experiments establish that these phonons have $T_1 < 10$ ps. From analysis of published Raman spectra and the linewidths, we infer that $T_1 > 2$ ps.[23(a),24] Using the density of states[5] we predict the most likely decay route of these phonons. The phonon frequencies and predicted decay routes are given in Table II. We can use this information and Eq. (6) to determine bounds on the $B$ coefficients for down conversion of these phonons, and we find them to lie in the range 0.2—0.6 $cm^{-1}$.

In the calculation of Della Valle *et al.*[21] of the $B$ coefficients of naphthalene, it was noted that the $B$ coefficients for the various decay pathways were nearly equal. These authors suggested the extreme complexity of the calculation could be avoided by a simplified model where these coefficients are assumed equal. This simplified model worked quite well for the organic molecular crystals naphthalene[14] and $l$-alanine[15] for a value $\langle B^{(3)} \rangle \approx 3\ cm^{-1}$. If we would apply the same model to $LaF_3$ we would choose an average $B$ coefficient of $\sim 0.3\ cm^{-1}$, an order of magnitude smaller than for the molecular crystals. This value would result in rough agreement with the low-temperature $T_1$'s of the phonons. However, it would not be in very good agreement with the detailed temperature dependence of the 78-$cm^{-1}$ phonon because it would predict a significant contribution from process 2 in Fig. 5.

The smaller value of $\langle B^{(3)} \rangle$ for $LaF_3$ ($\omega_D = 272\ cm^{-1}$) compared to naphthalene ($\omega_D = 90\ cm^{-1}$) and $l$-alanine ($\omega_D \approx 120\ cm^{-1}$) indicates that the lattice of this ionic crystal is significantly more harmonic than that of organic molecular crystals. This view is strengthened by comparison of available data on other measures of relative anharmonicity. Data on pressure-dependent phonon-frequency shifts at ambient temperature are available for $LaF_3$,[24] naphthalene,[28] and $\alpha$-glycine[29] (which is very similar to $l$-alanine). The proportional frequency shift $\Delta\nu/\nu$ from 0 to 5 kbar of the lowest-frequency Raman-active phonons are $\sim 1\%$ for $LaF_3$, $\sim 12\%$ for glycine, and $\sim 23\%$ for naphthalene. The coefficient of thermal expansion is also much smaller for $LaF_3$.[22,30]

The smallest $B$ coefficient we determine is for the process 78 $cm^{-1}$ + 78 $cm^{-1}$ → 156 $cm^{-1}$, process 2 in Fig. 5,

TABLE II. Predicted anharmonic decay pathways for emission at $T = 0$ K for phonons in $LaF_3$ observed by ps CARS.

| Phonon energy ($cm^{-1}$) | Decay pathway for emission ($cm^{-1}$) |
|---|---|
| 78 | 39+39 |
| 203 | 53+150 |
| 230 | 173+57 |
| 314 | 68+246 |
| 365 | 140+225 |
| 390 | 150+240 |

and it is less than 0.08 $cm^{-1}$. There appear to be two possible explanations for the absence of a significant contribution from this process. Although there is a considerable density of states at about 156 $cm^{-1}$, it is possible that $\vec{k}$-vector conservation cannot be satisfied. The density of states at $\sim 156$ $cm^{-1}$ most likely arises from the 145- or 166-$cm^{-1}$ ($\vec{k}=\vec{0}$ frequencies) phonons. It is possible that $\vec{k}$-vector conservation cannot be satisfied, which would occur, e.g., if both these phonons had dispersions which parallel the 78-$cm^{-1}$ mode. The other possibility is that there is a symmetry selection rule which governs phonon-phonon interactions in $LaF_3$, and possibly other crystals such as aragonite[23(b)] which also show small distortions away from a high-symmetry unit cell. In $LaF_3$ we have $B$ phonons which arise from the $D^4_{6h}$ bimolecular cell and $H$ phonons which are created from high-wave-vector $B$ phonons by the lattice distortion. The eigenvectors of the $H$ phonons do not belong to the irreducible representations of the $D^4_{6h}$ group, and consequently these phonons carry a property which the $B$ phonons do not, namely eigenvectors which transform according to the $D^4_{3d}$ factor group. This type of analysis has been previously called the mixed-factor–group model.[31] Once it is determined that the $H$ phonons possess a quantity the $B$ phonons do not, the selection rules are obvious. The $B$ phonons can decay by the process $B \rightarrow 2H$ since the emitted $H$ phonons are exactly out of phase. The up-conversion process $H+B \rightarrow H$ is similarly allowed, whereas the process $B+B \rightarrow H$ is forbidden since no interaction of two $B$ phonons can create an $H$ phonon. These selection rules are entirely consistent with our observations. This last rule makes an additional prediction, that $H$ phonons which can decay only by emission of $B$ phonons should be "bottlenecked" and have long lifetimes. We cannot observe such a bottleneck in $LaF_3$ because there are so many phonons that each $H$ mode has at least one allowed decay pathway. However, in simpler crystals like aragonite it is more likely that such a bottleneck can be observed.

## IV. SUMMARY

With the use of ps CARS, the vibrational dephasing rate of several $\vec{k}\approx\vec{0}$ optical phonons was studied in $LaF_3$:$Ce^{3+}$(2 at. %). $Ce^{3+}$-doped $LaF_3$ was studied because all previous work on high-frequency phonon dynamics in $LaF_3$ used doped crystals, and $Ce^{3+}$ shows no significant absorption at the wavelength of our lasers. The 78-$cm^{-1}$ mode has a nearly exponential ps CARS decay, yielding a lifetime of (380±20) ps at low temperature, corresponding to a Lorentzian Raman linewidth of (0.0140±0.0007) $cm^{-1}$. The other five phonons studied decayed with $T_1 < 10$ ps. Using published Raman data we can also set a lower bound of $T_1 > 2$ ps. The 78-$cm^{-1}$ mode decays into two optical phonons at 39 $cm^{-1}$. The cubic anharmonicity for this process is 0.15 $cm^{-1}$. For the decay of the other phonons, the anharmonicity is in the range 0.2–0.6 $cm^{-1}$. Thus the low-temperature data are in rough agreement with a simple model which assumes the anharmonic matrix element equal to an average value of $\sim 0.3$ $cm^{-1}$. However, the detailed temperature dependence obtained for the 78-$cm^{-1}$ mode would not be well fitted by this model because one process, 78 $cm^{-1} + 78$ $cm^{-1} \rightarrow 156$ $cm^{-1}$, has an anomalously small matrix element. We suggest there may be a selection rule for $LaF_3$ phonon-phonon scattering. This rule arises because $LaF_3$ has a nearly bimolecular unit cell with 21 optical phonons, but small distortions reduce the symmetry so there is actually a hexamolecular unit cell with 69 optical phonons.[25] If we let $B$ indicate a phonon which would exist in an ideal bimolecular crystal, and $H$ a phonon which exists only in the hexamolecular unit cell, these proposed rules may be summarized as follows:

$$B \rightarrow H + H, \quad H + B \rightarrow H, \quad B + B \not\rightarrow H .$$

We have demonstrated that the ps CARS technique is a powerful probe of high-frequency $\vec{k}\approx\vec{0}$ optical-phonon dynamics in low-temperature ionic crystals. The technique avoids the complication of indirect phonon generation and detection and the details of coupling surface excitations into the bulk crystal. Because the ps CARS decays are measured in the time domain, the lifetime and defect scattering contributions to the decay can be easily separated. It should be a straightforward technical matter to extend the technique to the subpicosecond regime, thus allowing detailed studies of the decay of very-high-frequency ($\omega \approx 3$ THz) optical phonons.

## ACKNOWLEDGMENTS

This work was supported by the National Science Foundation, Division of Materials Research, under Grant No. DMR-80-01630. D. D. D. acknowledges support from the Alfred P. Sloan foundation. We thank Jeffrey R. Hill for assistance in gathering the ps CARS data and Dr. Hargreaves of Optovac Inc. for providing $LaF_3$ and $LaF_3$:$Ce^{3+}$ crystals at no charge. Professor R. S. Meltzer, Professor G. S. Dixon, and Professor K. F. Renk kindly provided us with copies of unpublished work on $LaF_3$ phonon decay.

*Present address: Monsanto Corp., 800 N. Lindberg Blvd., St. Louis, MO 63167.

[1]C. H. Lee and D. Ricard, Appl. Phys. Lett. **32**, 168 (1977); B. H. Hesp and D. A. Wiersma, Chem. Phys. Lett. **75**, 423 (1980); K. Duppen, B. Hesp, and D. A. Wiersma, *ibid.* **79**, 399 (1981).

[2]F. Ho, W.-S. Tsay, J. Trout, and R. M. Hochstrasser, Chem. Phys. Lett. **83**, 5 (1981); F. Ho, W.-S. Tsay, J. Trout, S. Velsko, and R. M. Hochstrasser, *ibid.* **97**, 141 (1983).

[3](a) D. D. Dlott, C. L. Schosser, and E. L. Chronister, Chem. Phys. Lett. **90**, 386 (1982); (b) E. L. Chronister and D. D. Dlott, J. Chem. Phys. **79**, 5286 (1983); C. L. Schosser and D. D. Dlott, *ibid.* **80**, 1394 (1984).

[4]R. Reisfeld and C. K. Jørgensen, *Lasers and Excited States of Rare Earths* (Springer, Berlin, 1977).

[5]W. M. Yen, W. C. Scott, and A. L. Schawlow, Phys. Rev. **136**, A271 (1964).

[6]L. Erickson, Phys. Rev. B **16**, 4731 (1977).

[7]W. E. Bron, Rep. Prog. Phys. **43**, 301 (1980).
[8]A. Sher, R. Solomon, K. Lee, and M. W. Muller, Phys. Rev. **144**, 593 (1966).
[9]L. Godfrey, J. E. Rives, and R. S. Meltzer, J. Lumin **18-19**, 929 (1979).
[10]D. J. Sox, J. E. Rives, and R. S. Meltzer, Phys. Rev. B **25**, 5064 (1982).
[11]J. M. Will, W. Eisfeld, and K. F. Renk, Appl. Phys. A **31**, 191 (1983).
[12]R. S. Meltzer, J. F. Rives, and G. S. Dixon, Phys. Rev. B **28**, 4786 (1983).
[13]G. S. Dixon and R. M. Nicklow, Solid State Commun. **47**, 877 (1983).
[14]C. L. Schosser and D. D. Dlott, J. Chem. Phys. **80**, 1369 (1984).
[15]T. J. Kosic, R. E. Cline, and D. D. Dlott, Chem. Phys. Lett. **103**, 109 (1983).
[16]T. J. Kosic, R. E. Cline, and D. D. Dlott (unpublished).
[17]P. L. Decola, R. M. Hochstrasser, and H. P. Trommsdorff, Chem. Phys. Lett. **72**, 1 (1980).
[18]I. Abram, R. M. Hochstrasser, J. R. Kohl, M. G. Semack, and D. White, Chem. Phys. Lett. **52**, 1 (1977); I. Abram, R. M. Hochstrasser, J. E. Kohl, M. G. Semack, and D. White, J. Chem. Phys. **71**, 153 (1979).
[19]J. C. Bellows and P. N. Prasad, J. Chem. Phys. **70**, 1864 (1979).
[20]S. Califano, V. Schettino, and N. Neto, *Lattice Dynamics of Molecular Crystals* (Springer, Berlin, 1981).
[21]R. G. Della Valle, P. F. Fracassi, R. Righini, and S. Califano, Chem. Phys. **74**, 179 (1983).
[22]A. I. Kitaigorodsky, *Molecular Crystals and Molecules* (Academic, New York, 1973).
[23](a) R. P. Bauman and S. P. S. Porto, Phys. Rev. **161**, 842 (1967), and references cited therein; (b) M. A. Ismail, U. A. Jayasooriya, and S. F. Kettle, J. Chem. Phys. **79**, 4459 (1983).
[24]F. Cerdeira, V. Lemos, and R. S. Katiyar, Phys. Rev. B **19**, 5413 (1979).
[25]In the $D_{3d}^4$ structure, the 12 "$g$" fluorines are displaced by 0.059 lattice units, the 4 "$d$" fluorines by 0.063 lattice units, and the La ions by 0.0068 lattice from their positions in the bimolecular $D_{6h}^4$ structure [Ref. 23(a)].
[26]R. Laiho, M. Lakkisto, and T. Levola, Philos. Mag. A **47**, 235 (1983).
[27]B. DiBartolo, *Optical Interactions in Solids* (Wiley, New York, 1968).
[28]M. Nicol, M. Vernon, and J. T. Woo, J. Chem. Phys. **63**, 1992 (1975).
[29]J. A. Medina, W. F. Sherman, and G. R. Wilkinson, in C.R.—Conf. Int. Spectrosc. Raman, 7th, edited by W. F. Murphy (National Research Council of Canada, Ottawa, 1980), p. 112.
[30]W. Korczak and P. Mikołajczak, J. Cryst. Growth **61**, 601 (1983).
[31]U. A. Jayasooriya and S. F. A. Kettle, Phys. Rev. B **29**, 2227 (1984).